

Focus and Alignment Tolerance in a Photoconductive Terahertz Source

Gaudencio Paz-Martínez¹ · Jesus Garduño-Mejía¹ ·
Oleg V. Kolokoltsev¹ · Carlos G. Treviño-Palacios² ·
Naser Qureshi¹

Received: 30 March 2015 / Accepted: 24 June 2015 /
Published online: 9 July 2015
© Springer Science+Business Media New York 2015

Abstract Robust coupling between a pulsed laser beam and a photoelectric circuit is an important issue in the development of miniaturized, integrated, and embedded terahertz instrumentation. Here, we present a study of the effect of varying the focus and alignment parameters of an excitation laser pulse on the emission characteristics of a standard Hertzian-dipole type terahertz photoelectric source. The objective is to quantify the tolerance of a terahertz time-domain spectroscopy system, and we study the variation of peak amplitude, waveform, phase, and energy distribution as a function of excitation position and defocus. We find that a terahertz source can be made relatively tolerant to variations in focus, alignment, and details of the geometry of the photoelectric system, providing a window for a more robust field operation.

Keywords Photoconductive switch · Terahertz imaging · Terahertz source · Terahertz spectroscopy

1 Introduction

Spectroscopy and microscopy in the terahertz (THz) range of the electromagnetic spectrum has a great variety of applications in diverse areas of industry, science, and technology [1–6]. This has been possible in large part due to advances in the generation of THz waves, and the photoconductive switch has enjoyed widespread use in terahertz time-domain spectroscopy (THz-TDS) [1]. In current applications of terahertz spectroscopy and microscopy, robust

✉ Naser Qureshi
naser.qureshi@ccadet.unam.mx

¹ Centro de Ciencias Aplicadas y Desarrollo Tecnológico (CCADET), Universidad Nacional Autónoma de México, Mexico, Distrito Federal, Mexico

² Instituto Nacional de Astrofísica, Óptica y Electrónica, (INAOE), Tonantzintla, Puebla, Mexico

integration of optics and terahertz circuitry has taken on an important role, especially in the development of compact THz-TDS instruments [7] for field work or for embedded sensors where manual alignment and maintenance is not an option.

Starting with Auston et al.'s work [8], numerous advances in terahertz generation using the photoconductive antenna method resulted from optimizing antenna structures [9]. For example, the use of sharp electrodes to create electric field singularities [10] or more complex systems such as plasmonic contact electrodes for increasing the quantum efficiency [11] has been used to increase power output. The details of the location of illumination have also been shown to affect radiation properties [12] but have received somewhat less attention. It has been shown, for example, that in addition to antenna structure, the exact illumination position [13, 14] and form [15] affect the resultant terahertz wave. One reason for this is the space-charge screening effect [16, 17], and it has been shown that a suitable illumination spot shape, for example, an elliptical spot [18], can significantly mitigate screening and improve the emission spectrum and power.

In this work, we seek to contribute to a clearer understanding of the effect of small changes in the laser excitation and map out in detail the effect of illumination position and spot size in a systematic way. Here, we use a standard illumination scheme where a laser beam is focused to a circular spot. We scan the complete H-shaped structure of a standard photoelectric terahertz source with a pulsed laser spot, in a setup similar an LTEM microscope [19] but using the emitter itself as a sample, and at each point record the terahertz electric field in the time domain using a photoelectric antenna structure as detector. An analysis of the peak amplitude, time evolution of the wave, and energy distribution is performed in selected regions of H-shaped structure. We scan the laser spot in focus and then defocus the spot in a controlled manner and look at the effect on the THz radiation parameters. We map out the regions of maximum emission efficiency and find regions where the emission characteristics are relatively insensitive to variations in the laser excitation parameters, providing a set of parameters for relatively robust operation in non-ideal operational conditions.

2 Experimental

The experimental setup is shown in Fig. 1. A mode locked Ti:sapphire laser with 150 femtosecond pulse width was used to excite a photoelectric switch at a wavelength of 800 nm and a 76 MHz repetition rate. The laser was focused using an aspheric lens that achieves a 5- μm spot size when in focus. The emitter was a 20- μm -long gold dipole patterned on low temperature gallium arsenide (LT-GaAs, manufactured by Menlo Systems), and an identical structure was used as detector in a standard time-domain spectroscopy (THz-TDS) configuration [1]. Spherical silicon lenses were attached at the emitter to partially collimate [20] the terahertz radiation and at the detector to capture the radiation. The detector was placed a few millimeters from the emitter.

The experiment was carried out by scanning the emitter antenna structure in two dimensions, while the excitation laser spot was fixed in the same position. Two types of scans were performed: one fast and the other slow. In the first case, only the peak amplitude of the emitted THz pulse was measured in order to form a peak intensity map as a function of excitation position on the antenna. In the second case, the entire shape of THz pulse was obtained in the time domain at each pixel by scanning the delay between the THz source excitation pulse and the detection pulse. For the case of the fast scan, each pixel was set at 2.5 μm and the scan area

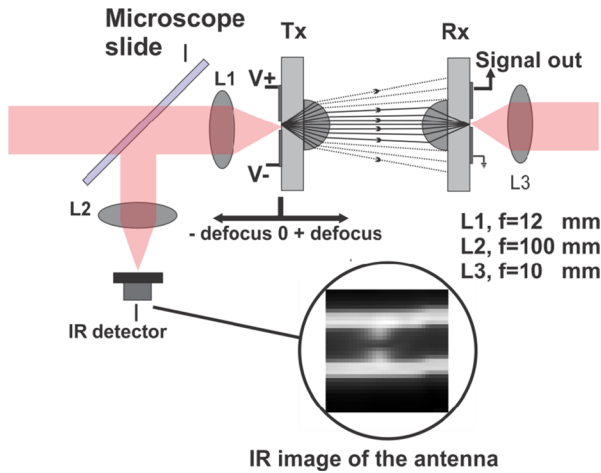


Fig. 1 Experimental setup. An LT-GaAs photoelectric terahertz source is spatially scanned in three dimensions as the emitted THz radiation is detected in a standard time-domain spectroscopy setup

was $80 \times 80 \mu\text{m}$. Scans were performed when the laser was in focus, and then the antenna was moved forward and backward from its focus position in order to vary the spot size. For the case of the slow scan, the scan area was identical but each step in the scan (or pixel size) was set to $7.5 \mu\text{m}$ in order to keep data acquisition times within reasonable limits. The excitation laser power was maintained at 9 mw.

A microscope slide was used to sample some of the light reflected from the photoconductive emitter during the scan, and this light was focused onto a silicon photodiode (Fig. 1). In this way, a simultaneous optical reflectivity image of the antenna was obtained, allowing us to correlate the terahertz emission map with the physical structure of the antenna.

3 Results

Firstly, we quantify the defocus tolerance. Figure 2 shows the peak amplitude of the terahertz pulse versus defocus distance. The minimum spot size was $5 \mu\text{m}$, and the Rayleigh length for the optical lens was $98 \mu\text{m}$. The most useful observation here is that there is a range of about $250 \mu\text{m}$, more than two Rayleigh lengths, in which the output power of the terahertz emitter is almost flat. After a defocus of 3 Rayleigh lengths, the maximum of THz signal has drop to half.

Next, we quantify the defocus tolerance and include the effect of changing the center position of the excitation spot in the plane of the emitter. Figure 3 shows series maps of THz peak amplitude as a function of excitation position in two dimensions, each taken at a different defocus distance. For clarity, the position of H-shaped antenna is drawn over the map. When the laser is in focus, the largest THz signal is found when the antenna structure is excited near the dipole gap, as is well known. However, there is still a significant terahertz emission when the structure is illuminated between transmission lines, far from the dipole. Interestingly, there is a signal, albeit smaller, when the structure is illuminated *above* or *below* the transmission lines. This is likely related to carrier injection [21] and the short distance between transmission lines. Effectively, there is a large region, of the order of $50 \mu\text{m}$, even with a small spot size of

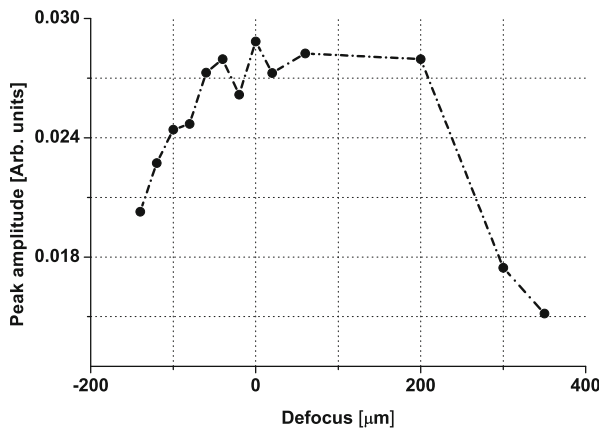


Fig. 2 Peak amplitude of the terahertz pulse as a function of defocus in the optimal excitation spot. The spot size is 5 μm and the Rayleigh length is 98 μm

5 μm , over which the structure can be illuminated and produces a readily measurable THz signal. When the spot is defocused up to about 200 μm (2 Raleigh lengths), significant THz emission is achieved over a larger area close to the dipole gap, as one would expect. At defocus distances above 200 μm , THz radiation is generated by illuminating over a much greater area, and we observe a peculiar lobe structure in the distribution. This can be understood as a convolution of the diffracted optical beam (which has a ring structure) with the antenna shape. We do not see a sharp increase in emission at the very edges of the dipole, which indicates that the trap enhancement effect near the anode [21, 22] is not important.

The effect of illumination position on the THz spectrum was also quantified. Figure 4 shows time-resolved measurements of the THz wave at selected points on the antenna structure when the excitation spot is optimally focused. In each row, the color line indicates the exact

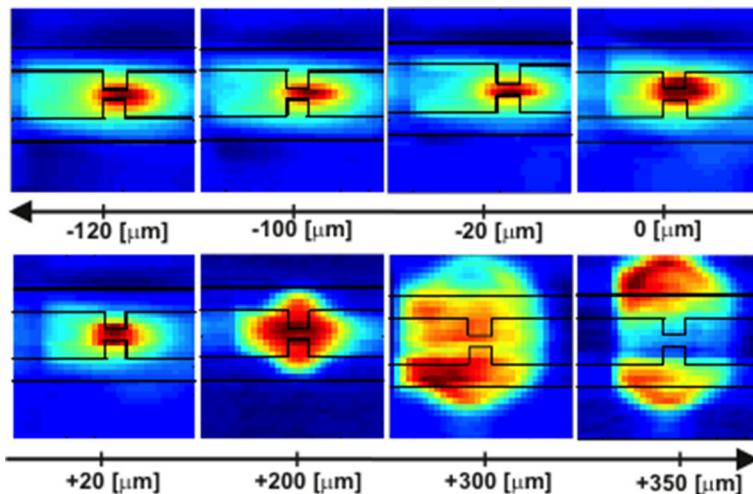


Fig. 3 Normalized map of the distribution of peak THz amplitude along the H-shaped structure for selected distances of defocus in the optical excitation, in a range of about five Raleigh lengths. Red indicates high amplitude and blue indicates low amplitude

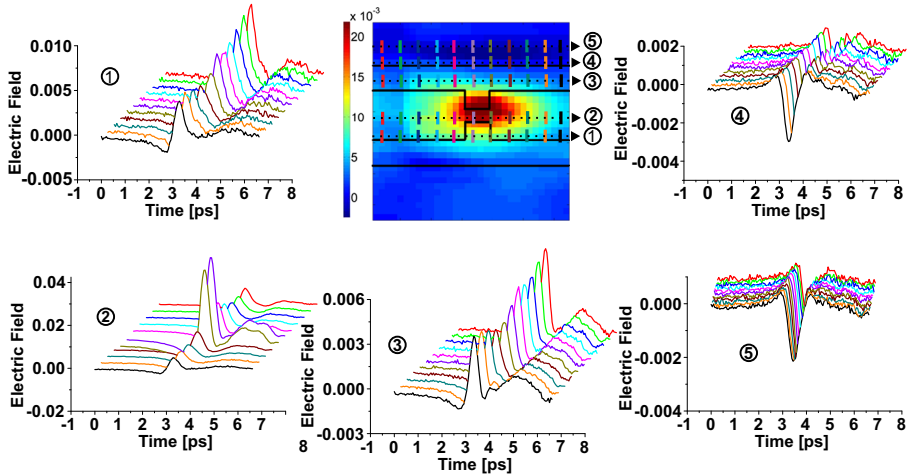


Fig. 4 Time-resolved electric field measurements of the THz wave when the emitter is illuminated at selected points with the laser in focus. Curves have been offset for clarity. The actual time value of the peak electric field does not change with position, and the electric field scale is arbitrary but comparable directly with Figs. 5 and 6

place where the center of the laser spot hits the emitter, starting from the left with red on the left to black on the right of the scan area. When the defocus is 0, line 2 passing through the center of the gap is found to contain the pulse with maximum amplitude, corresponding to THz emission in the center of the gap. This is the optimal excitation condition. Far from the gap, the peak amplitude drops significantly, but the form of the wave in the time domain does not change drastically. There is, therefore, a significant range of tolerance in the exact point at which the antenna is illuminated in which the THz wave is virtually unchanged. This is a non-trivial observation, in that we can change the point of illumination without changing the effective shape of the antenna. The data indicate that the emission spectrum is not strongly dependent on whether we illuminate the dipole or simply illuminate between two transmission lines.

Interestingly, when we illuminate outside of the transmission line area (i.e., above the H-shape), the phase of the THz wave changes abruptly by 180° as seen in lines 4 and 5, but the amplitude of this signal is small compared to the amplitude generated at the dipole center. This can be understood as a change in the direction of the bias electric field surrounding the transmission line structure. The contribution of this effect to the overall emission is small.

It is instructive to repeat this exercise at 200 μm of defocus (2 Rayleigh lengths), when the peak emitted power is still flat as a function of defocus. The result is shown in Fig. 5: the pulse shape is very similar to that in Fig. 4, and we see the same general behavior at different illumination points. However, the peak amplitude of the pulses begins to have a more uniform distribution near the gap compared to the focused case. In other words, we observe that the general shape of the THz wave does not change significantly with two Rayleigh lengths of defocus.

In a more extreme case of defocus, shown in Fig. 6, we see the result for a defocusing distance of 300 μm (3 Rayleigh lengths). The THz signal characteristics become very insensitive to the illumination position over a large area, the amplitude of electric field decreases almost four times compared to the maximum value when the laser is in focus

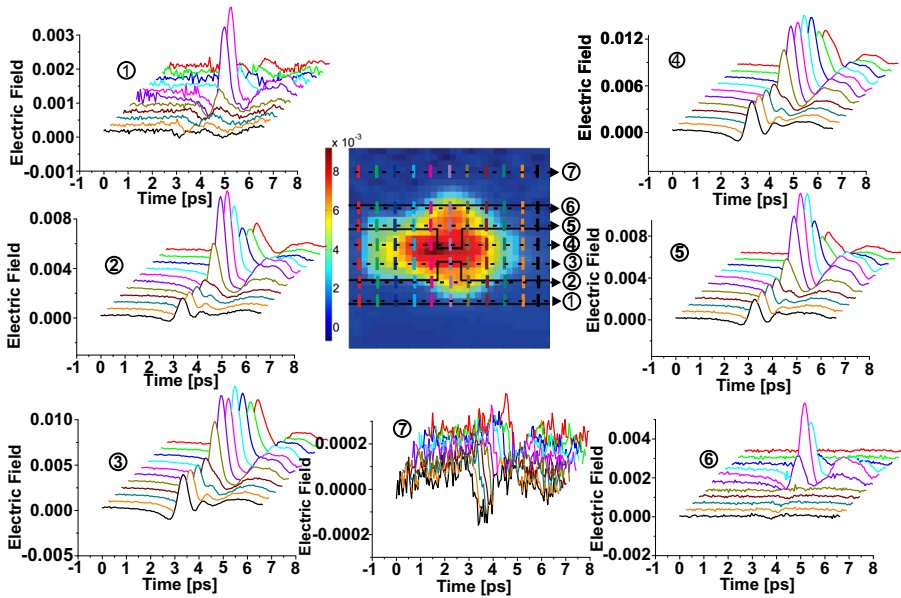


Fig. 5 Time-resolved electric field measurements of the THz wave when the emitter is illuminated at selected points with 200 μm of defocus

(consistent with Fig. 1), and the phase change effect in Fig. 4 disappears. The important point here is that with such an extreme defocus, we gain tolerance in the THz wave form and lose output power (as one would intuitively expect).

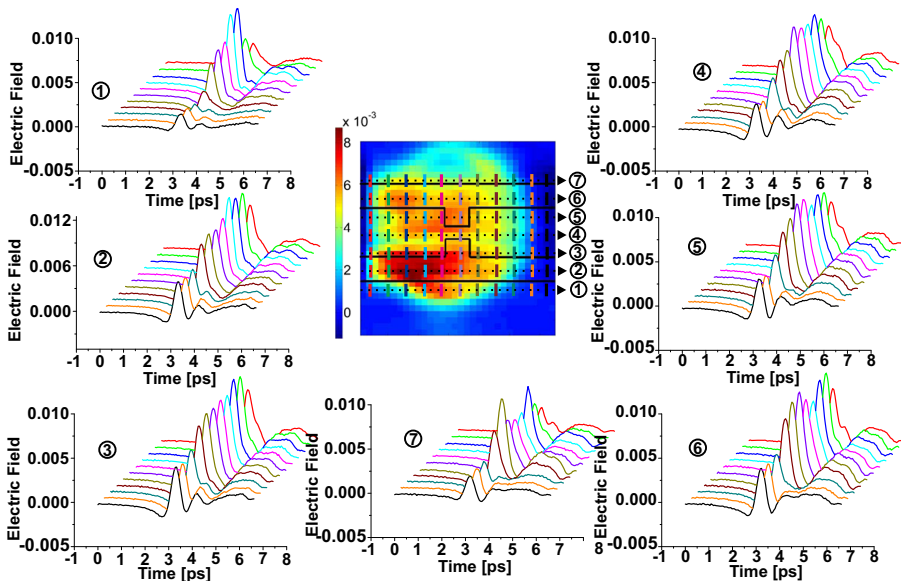


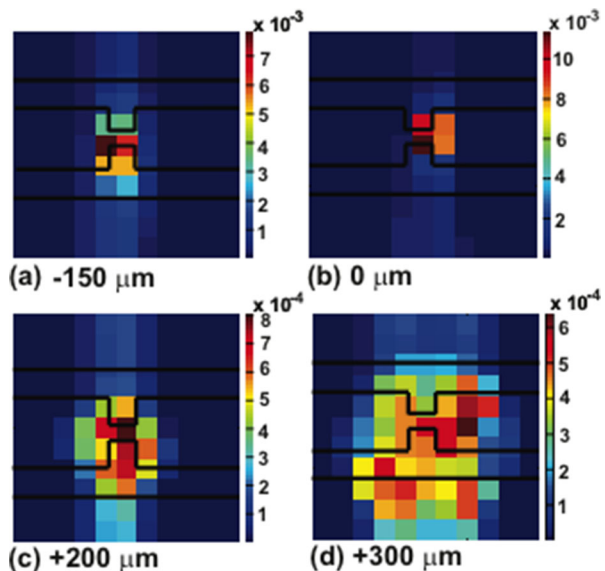
Fig. 6 Time-resolved electric field measurements of the THz wave when the emitter is illuminated at selected points with 300 μm of defocus

To quantify the efficiency of the THz emitter, Fig. 7 shows a map of energy distribution. Here, each pixel is $7.5 \mu\text{m}$ and each image covers an $80 \times 80 \mu\text{m}$ area and the total energy was calculated using the Parseval's theorem. It is interesting to note that the efficiency of THz generation suffers very little change when the system has a defocus of 1.5 Rayleigh lengths (Fig. 7a, b). At 2 to 3 Rayleigh lengths of defocus, the efficiency falls by a factor of 10 (Fig. 7c, d), and the energy is distributed in a region that covers the transmission lines and the dipole (Fig. 7d). This is an interesting result because it indicates that terahertz radiation may be generated in several regions of an antenna structure and these signals contribute to the total THz signal radiated into free space. The signal at 180° out of phase that is observed in Fig. 4, on top of H-shape (anode), is not a problem because it is a very small signal and its effect is small.

4 Conclusions

We have mapped the effect of defocusing and varying the illumination position on a standard LT-GaAs photoelectric terahertz source. We find a region of about 2 Rayleigh lengths of defocus where the system is relatively tolerant to defocusing the illumination beam, and there is little change in the peak power when illuminated at the center of the emission dipole. The exact illumination position has an observable but relatively small effect on the details of the emission spectrum, revealing a surprising insensitivity to the effective shape of the emitter. At 3 Rayleigh lengths of defocus, the efficiency of generation falls an order of magnitude, the peak amplitude a factor of approximately four and this changes very little when the center position of the illumination beam is scanned over an area of $80 \mu\text{m}$. At 1.53 Rayleigh lengths of defocus, the emitted terahertz radiation has similar parameters to the focused case, and a good tolerance to defocus. These parameters can be used to reduce the cost of a TDS system: instead of using a costly linear stage for fine focusing, a cheaper linear stage can be used.

Fig. 7 Energy distribution of the emitted radiation as a function of excitation position. The energy scale is arbitrary but are the same for maps (a–d) which correspond to defocus distances from -150 to $300 \mu\text{m}$



Acknowledgments This work was supported by grants PAPIIT IN104513 and IG100615 from Universidad Nacional Autónoma de México.

References

1. P. Uhd Jepsen, D. G. Cooke and M. Koch, “Terahertz spectroscopy and imaging – Modern techniques and applications”, *Laser Photonics Rev.* 5, No. 1, 124–166 (2011).
2. D. Grischkowsky, S. Keiding, M. Van Exter, and Ch. Fattinger, “Far-infrared time-domain spectroscopy with terahertz beams of dielectrics and semiconductors”, *J. Opt. Soc. Am. B* 7, 2006–2015 (1990).
3. W. L. Chan, J. Deibel, D. M. Mittleman, “Imaging with terahertz radiation”, *Rep. Prog. Phys.* **70** 1325–1379, (2007).
4. K. Ishihara, K. Ohashi, T. Ikari, et al., “Terahertz-wave near-field imaging with subwavelength resolution using surface-wave-assisted bow-tie aperture”, *Appl. Phys. Lett.*, vol. 89, 201120, (2006).
5. R. Kersting, et al., “Terahertz near-field microscopy”, *Advances in Solid State Physics*, R. Haug, Editor. 2008, Springer-Verlag Berlin: Berlin. p. 203–222
6. A. J. Huber, F. Keilmann, J. Wittborn, J. Aizpurua, and R. Hillenbrand, “Terahertz Near-Field Nanoscopy of Mobile Carriers in Single Semiconductor Nanodevices”, *Nano Letters* 8 (11), 3766–3770 (2008).
7. N. Vieweg, F. Rettich, A. Deninger, H. Roehle, R. Dietz, T. Göbel, M. Schell, “Terahertz-time domain spectrometer with 90 dB peak dynamic range”, *J Infrared Milli Terahz Waves* 35:823–832 (2014).
8. D. H. Auston, K. P. Cheung, P. R. Smith, “Picosecond photoconducting Hertzian Dipoles”, *Appl. Phys. Lett.* **45**, 284 (1984).
9. Fumiaki Miyamaru, Yu Saito, Kohji Yamamoto, Takashi Furuya, Seizi Nishizawa, and Masahiko Tani, “Dependence of emission of terahertz radiation on geometrical parameters of dipole photoconductive antennas”, *Appl. Phys. Lett.* 96, 211104 (2010).
10. Y. Cai, I. Brener, J. Lopata, J. Wynn, L. Pfeiffer, J. Federici, “Design and performance of singular electric field terahertz photoconducting antennas”, *Appl. Phys. Lett.*, vol. 71, No. 15, pp. 2076–2078 (1997).
11. C. W. Berry, N. Wang, M. R. Hashemi, M. Unlu, and M. Jarrahi, “Significant performance enhancement in photoconductive terahertz optoelectronics by incorporating plasmonic contact electrodes”, *Nature Communications* 4, 1622, (2013).
12. N. Khiabani, Y. Huang, and Yao-chun Shen, “Discussions on the main parameters of THz photoconductive antennas as emitters”, *Proceedings of the 5th European Conference on Antennas and Propagation*, (2011).
13. Ian S. Gregory, Colin Baker, William R. Tribe, Ian V. Bradley, Michael J. Evans, Edmund H. Linfield, A. Giles Davies, and Mohamed Missous, “Optimization of Photomixers and Antennas for Continuous-Wave Terahertz Emission”, *IEEE Journal of Quantum Electronics*, 41, 717, (2005).
14. M. Tani, S. Matsuura, K. Sakai, and S. Nakashima, “Emission characteristics of photoconductive antennas based on low-temperature-grown GaAs and semi-insulating GaAs”, *Appl. Opt.* 36, 7853–7859 (1997).
15. J. H. Kim, A. Polley, S. E. Ralph, “Efficient photoconductive terahertz source using line excitation”, *Opt. Lett.*, 30, 2490 (2005).
16. P. Uhd Jepsen, R. H. Jacobsen, and S. R. Keiding, “Generation and detection of terahertz pulses from biased semiconductor antennas”, *J. Opt. Soc. Am. B*/Vol. 13, 2424 (1996).
17. Z. Piao, M. Tani and K. Sakai, “Carrier dynamics and terahertz radiation in photoconductive antennas”, *Jpn. J. Appl. Phys.* Vol. 39 (2000) pp. 96–100.
18. D. S. Kim, D. S. Citrin, “Enhancement of terahertz radiation from photoconductors by elliptically focused excitation”, *Appl. Phys. Lett.*, 87, 061108, (2005).
19. H. Murakami, N. Uchida, R. Inoue, S. Kim, T. Kiwa and M. Tonouchi, “Laser Terahertz Emission Microscope”, *Proceedings of the IEEE* 12, 1646 (2007).
20. J. Van Rudd and D. M. Mittleman, “Influence of substrate-lens design in terahertz time-domain spectroscopy”, *J. Opt. Soc. Am. B*, 19 (2), 319 (2002).
21. S. E. Ralph, D. Grischkowsky, “Trap-enhanced electric fields in semi-insulator: The role of electrical and optical carrier injection”, *Appl. Phys. Lett.*, 59, 1972 (1991).
22. I. Brener, D. Cykaar, A. Frommer, L. N. Pfeiffer, J. Lopata, J. Wynn, K. West, and M.C. Nuss, “Terahertz emission from electric field singularities in biased semiconductors”, *Optics Letters*, 21, 1924 (1996)